Effect of Intermolecular Forces on the Static and Dynamic Performance of Air Bearing Sliders: Part II– Dependence of the stability on Hamaker constant, suspension preload and pitch angle.

Vineet Gupta

Graduate Student

Department of Mechanical Engineering

University of California, Berkeley

email: vineet@cml.me.berkeley.edu

David B Bogy

William S. Floyd, Jr., Distinguished Professor in Engineering

Department of Mechanical Engineering

University of California, Berkeley

email: dbogy@cml.me.berkeley.edu

ABSTRACT

Intermolecular and surface forces contribute significantly to the total forces acting on air bearing sliders for flying heights below 5nm. Their contributions to the total force increase sharply with the reduction in flying height, and hence their existence can no longer be ignored in air bearing simulation for hard disk drives. Various experimentally observed dynamic instabilities can be explained by the inclusion of these forces in the model for low flying sliders. In this paper parametric studies are presented using a 3-DOF model to better understand the effect of the Hamaker constants, suspension pre load and pitch angle on the dynamic stability/instability of the sliders. A stiffness matrix is used to characterize the stability in the vertical, pitch and roll directions. The fly height diagrams are used to examine the multiple equilibriums that exist for low flying heights. It has been found that the system instability increases as the magnitude of the van der Waals force increases. It has also been found that higher suspension pre load and higher pitch angles tend to stabilize the system.

NOMENCLATURE

The values in the parentheses are the typical values used in this study.

C, D	: constants for atoms in vacuum (10^{-77} Jm^6, 10^{-134} Jm^{12})
U(z)	: Total pair potential
ρ_1, ρ_2	: the number densities of atoms in the disk and the slider respectively
A	: Hamaker constant, $A = \pi^2 C \rho_1 \rho_2$ (10^{-19} J)
B	: Constant, $B = \pi^2 D \rho_1 \rho_2$ (10^{-76} Jm^6)
z	: fly height, nm
θ	: pitch angle, μrad
φ	: roll angle, μrad
m	: slider's mass, gm
I_θ, I_φ	: slider's moments of inertia in pitch and roll directions, respectively
F_{su}	: suspension pre load, gm
F_c	: contact force, gm
F_{vdw}	: intermolecular force, gm
$M_{su\theta}$, $M_{su\varphi}$	: moment in the pitch and roll directions due to suspension preload
$M_{sh\theta}$, $M_{sh\varphi}$	: moment in the pitch and roll directions due to shear force
$M_{c\theta}$, $M_{c\varphi}$	: moment in the pitch and roll directions due to contact force
$M_{vdw\theta}$, $M_{vdw\varphi}$	: moment in the pitch and roll directions due to intermolecular force
p	: air pressure, Pa
p_a	: ambient pressure, Pa (1.01325×10^5 Pa)
P	: dimensionless air pressure, p/p_a

H	: dimensionless bearing clearance, h/h_m
X	: dimensionless coordinate in slider length direction, x/L
Y	: dimensionless coordinate in slider width direction, y/L
h_m	: reference clearance at the trailing edge center, nm
L	: length of the slider, mm
Λ_x	: bearing number in x direction, $6\mu UL/p_a h_m^2$
Λ_y	: bearing number in y direction, $6\mu VL/p_a h_m^2$
σ	: squeeze number, $12\mu\omega L^2/p_a h_m^2$
Q	: flow factor, assumes different forms depending on the type of slip model used
F	: total force in z direction
T_θ, T_φ	: total torque in the pitch and roll directions, respectively
ID, MD, OD	: Inner diameter, middle diameter and outer disk diameters, respectively

INTRODUCTION

In order to achieve an areal density goal of 1Tbit/in^2, the magnetic spacing between the slider and the disk has to be reduced to below 10nm. Such low magnetic spacing translates to even lower mechanical spacing of 5nm or less. Certain physical phenomena, such as intermolecular and surface forces that did not have significant effect on the flying characteristics of the higher flying sliders in earlier technologies, now become increasingly important as the slider fly height reduces. These forces are attractive in nature for mechanical spacings as low as inter-atomic separations (0.4nm). Their attractive nature results in a reduction of the mechanical spacing [2, 4]. Since these forces are highly non linear, they result in dynamic instability of the slider at low fly heights, which has also been observed experimentally [3, 5]. Hence the existence of intermolecular and surface forces and the induced dynamic instability at low separations can no longer be ignored. A parametric study was previously conducted using a single DOF model to predict the effect of intermolecular force (IMF), disk topography and air bearing stiffness and damping on the instability at the head disk interface [5, 9]. However these models were unable to predict all of the complex dynamic instabilities since the effects of the pitch and roll angles were not considered. A 3-DOF air bearing model is used in this parametric study to characterize the effect of the Hamaker constant, suspension pre load and pitch angle on the dynamic stability/instability of the HDI due to intermolecular forces.

INTERMOLECULAR FORCE BETWEEN TWO LAYERS

The total intermolecular forces include attractive and repulsive forces. The attractive forces are quantum mechanical in origin and they act between all atoms and molecules, even if they are totally neutral. But the resulting interaction is a quantum mechanical polarization which is electrostatic in nature. The repulsive forces at small intermolecular separations are due to overlap of the electron clouds of the atoms. These forces determine how close two atoms or molecules may approach each other.

The total pair potential obtained by summing the attractive and repulsive potentials is often modeled using the Lennard-Jones or ‘6-12’ potential formulation

$$U(z) = -\frac{C}{z^6} + \frac{D}{z^{12}} \qquad (1)$$

where *C* and *D* are constants for atoms in vacuum. In order to calculate the van der Waals interaction energies in vacuum for a pair of bodies of different geometries, we assume that the interaction is non-retarded and additive. The total interaction energy between the slider and the disk, obtained by integrating the above expression over the slider surface, is given by

$$U_{tot}(z) = -\frac{A}{12\pi}\iint\limits_{\substack{\text{Rect}\\ area}} \frac{dxdy}{z^2} + \frac{B}{360\pi}\iint\limits_{\substack{\text{Rect}\\ area}} \frac{dxdy}{z^8} \qquad (2)$$

where $A = \pi^2 C\rho_1\rho_2$ and $B = \pi^2 D\rho_1\rho_2$ in which ρ_1 and ρ_2 are the number densities of atoms in the disk and the slider, respectively. Typical values for *A* and *B* are about 10^{-19} J and 10^{-76} Jm^6 , respectively. The intermolecular forces between the slider and the disk, obtained by differentiating the potential, can be written as

$$F_{vdw} = \frac{d(U_{tot})}{dz} = -\frac{A}{6\pi}\iint\limits_{\substack{\text{Rect}\\ area}} \frac{dxdy}{z^3} + \frac{B}{45\pi}\iint\limits_{\substack{\text{Rect}\\ area}} \frac{dxdy}{z^9} \qquad (3)$$

INTERMOLECULAR FORCE MODELING

When the slider is flying at sufficiently low mechanical separations the significant forces acting on the slider at the HDI are the suspension force, air bearing force, contact force, shear force and the intermolecular force.

To calculate the static flying characteristics of the air bearing slider, we considered a 3 DOF model in the variables fly height (z), pitch (θ) and roll (φ). The following force and moment balance equations are used to model the HDI

$$\begin{aligned} m\frac{d^2z}{dt^2} &= F_{su} + F_c + F_{vdw} + \int (p - p_a)dA \\ I_\theta\frac{d^2\theta}{dt^2} &= M_{su\theta} + M_{sh\theta} + M_{c\theta} + M_{vdw\theta} + \int (p - p_a)(x_g - x)dA \\ I\varphi\frac{d^2\varphi}{dt^2} &= M_{su\varphi} + M_{sh\varphi} + M_{c\varphi} + M_{vdw\varphi} + \int (p - p_a)(y_g - y)dA \end{aligned} \qquad (4)$$

The relationship between the pressure distribution and the HDI spacing is given by the generalized Reynolds equation.

$$\frac{\partial}{\partial X}\left(QPH^3\frac{\partial P}{\partial X}-\Lambda_x PH\right)+\frac{\partial}{\partial Y}\left(QPH^3\frac{\partial P}{\partial Y}-\Lambda_y PH\right)=\sigma\frac{\partial}{\partial t}(PH) \qquad (5)$$

These equations are used to calculate the dynamic response of the air bearing slider. The Quassi-Newton iteration method is implemented to calculate the static solutions, the case where all the time dependent terms are zero.

STABILITY CRITERIA FOR THE HDI

For stability of the HDI, the total stiffness in the vertical, pitch and roll directions must be positive. In other words the total bearing load capacity must be positive. It has been found that at ultra low fly heights the z-stiffness value decreases as the fly height decreases and becomes negative below a critical fly height value. Negative stiffness means that the bearing is unable to maintain a mechanical spacing between the slider and the disk, which leads to contact between the slider and the disk.

The stiffness matrix relating changes in the forces in the z direction and moments in the pitch and roll directions to the changes in the fly height (z), pitch (θ) and roll (φ) can be mathematically represented as

$$\begin{bmatrix} dF \\ dT_\theta \\ dT_\varphi \end{bmatrix} = \begin{bmatrix} \frac{\partial F}{\partial z} & \frac{\partial F}{\partial \theta} & \frac{\partial F}{\partial \varphi} \\ \frac{\partial T_\theta}{\partial z} & \frac{\partial T_\theta}{\partial \theta} & \frac{\partial T_\theta}{\partial \varphi} \\ \frac{\partial T_\varphi}{\partial z} & \frac{\partial T_\varphi}{\partial \theta} & \frac{\partial T_\varphi}{\partial \varphi} \end{bmatrix} \begin{bmatrix} dz \\ d\theta \\ d\varphi \end{bmatrix} \qquad (6)$$

where $\partial F / \partial z = 1$ unit means 1 unit of force is needed to change the fly height by 1 unit.

As discussed in the Part I paper [1] the system is stable only if it is stable in all three directions, i.e. z, pitch and roll. Mathematically, if all three eigenvalues of the stiffness matrix are positive, then the system is stable. But if one or more of the eigenvalues of the stiffness matrix are negative, then the system is unstable.

STABILITY PREDICTION USING THE FLY HEIGHT DIAGRAMS

In this study the stability/instability of the HDI was analyzed using a “fly height diagram” as presented in Part I paper [1]. The fly height diagram plots the slider fly height versus disk rpm. The minimum mechanical spacing between the slider and the disk is referred to as the fly height. A typical fly height

diagram is shown in fig.1. The greater the rpm range of the unstable region, the higher will be the hysterisis observed in the touchdown-takeoff experiments. A detailed description of the fly height diagram is given in the Part I paper [1].

EFFECT OF THE MAGNITUDE OF VAN DER WAALS FORCES ON THE STABILITY OF THE HDI

Like gravitational forces, the dispersion forces act between all atoms and molecules, even if they are neutral. But unlike gravitational forces, these forces are not generally pair-wise additive. The force between any two molecules is affected by the presence of other molecules nearby. This is because the field emanating from any one molecule reaches the second molecule both directly and by reflection from other molecules since they too are polarized by the field. The problem of non additive nature of dispersion forces is completely avoided by Lifshitz Theory where the atomic structure is ignored and the forces between the large bodies – treated as continuous media – are derived in terms of such bulk properties as dielectric constants and refractive indices [7].

The multiple layers at the head disk interface cannot be treated as bulk material. And also the changes in the thickness and the material properties of the lubricant and the head-disk overcoats change the magnitude of the total intermolecular force. To analyze the effect this has on the stability of the system, we considered three different values of the Hamaker constant $A_1 = 0.5*10^{-19}$ J, $A_2 = 10^{-19}$ J, $A_3 = 2*10^{-19}$ J. Static simulations were performed using the 3-DOF air bearing model to calculate the steady state fly height for the slider shown in fig.2.

A multi-equilibrium region is shown using the fly height diagram in fig.3. It is seen that as the value of the Hamaker constant increases from A_1 to A_3, the rpm range of the unstable region also increases from 1400 to 3800. Therefore, for higher values of the Hamaker constant, more hysterisis will be observed in touchdown-takeoff experiments and hence the system has more instability. The desired fly heights for various values of the Hamaker constant are shown in Table 1. We observe that the desired fly height also increases from 4.08 nm to 5.39 nm with the increase in the Hamaker constant from A_1 to A_3, which in turn limits the areal density that can be achieved.

EFFECT OF THE PITCH ANGLE ON THE STABILITY OF THE HDI

Static simulations were performed for the slider design shown in fig.2 for three different radial positions. The fly height diagram (fig.4) shows the equilibrium fly heights at the three radial positions. We observe that the rpm range of the unstable region is least at the outer diameter (OD) position and greatest at the inner diameter (ID) position. The desired fly height also decreases from ID (6.07nm) to MD (5.07nm) to OD (3.57nm) as shown in Table 2.

A stable fly height of 4 nm is greater than the desired fly height value at the OD (3.57 nm), but is less than the corresponding value at the MD (5.07 nm) and the ID (6.07 nm) radial positions. With reference to the earlier discussion in the Part I paper [1], we can conclude that for a stable fly height of 4 nm, the system will be stable at the OD, but it will undergo large fly height modulations at ID and MD positions if the slider is perturbed from its stable equilibrium position. This perturbation can be due to many factors such as air flow, disk roughness, etc.

Figure 5 shows the relationship between the stable pitch angle and the stable fly height. We observe that the pitch angle at the OD (190 μrad) is much larger than the pitch angles at the ID (80 μrad) and MD (90 μrad) positions for a stable fly height of 4nm. Thus we observe that higher pitch angles are desired to increase the stability of the system. This can be explained due to the fact that for higher pitch angles (with the same stable fly height), less area of the slider is close to the disk surface and hence the intermolecular attraction between the slider and the disk is reduced. It has been shown in the previous section that as the magnitude of the intermolecular force decreases (i.e. equivalent to saying that the values of the Hamaker constant decreases), the slider becomes more stable.

To analyze the effect of the slider form factor on the stability, static simulations were performed for pico and femto designs at the same radial positions for the sliders shown in fig.6. The pico slider was simulated with 1.5gm suspension load and the femto slider was simulated with 0.75gm and 1.5gm suspension loads. The multi-equilibrium region is shown in the fly height diagram in fig.7. Figure 8 plots the variation of the stable pitch angle with the stable fly height. As discussed earlier we observe that higher pitch angles result in more dynamic stability of the system.

EFFECT OF SUSPENSION LOAD ON THE STABILITY OF THE HDI

To analyze the effect of the slider form factor on the stability of the HDI, static simulations for the femto design were carried out at two different suspension preload values. This was done for two different slider designs. It was observed in both cases that lower stable fly heights can be achieved with higher suspension preloads. Hence it is important to study the effect of suspension preload on the stability of the system.

Static simulations at five different suspension preload values (varying from 1gm to 3gm) were done for the pico design at the same radial position for the slider shown in fig.2. The fly height diagrams are shown in fig.9. We observe that the pico designs with higher suspension preloads have smaller unstable rpm range. Hence less hysterisis will be observed with higher suspension preloads in touchdown-takeoff simulations. The desired fly height for the five cases is shown in Table 4. For a suspension preload of 1gm the desired fly height is 4.44 nm at a disk rpm of 3100, which reduces to a desired fly height of 1.87 nm at a disk rpm of 7600 for a suspension preload of 3gm. Thus a higher suspension preload results in a smaller desired fly height. It can be concluded from the above simulations that increasing the preload decreases the desired fly height value, but we need to spin the disk at higher rpm's to attain this fly height. Fig.10 shows the variation of the stable pitch angle with the stable fly height. As discussed earlier we again observe that higher pitch angles result in greater dynamic stability of the system.

CONCLUSION

Intermolecular forces are included in the CML static and dynamic air bearing design programs. Static simulations are carried out with and without considering intermolecular forces. A higher Hamaker constant for the interface layers results in an increased magnitude of the intermolecular forces and hence a more unstable system. The desired fly height also increases with the increase in Hamaker constant, which in turn limits the areal density that can be achieved. We also conclude that higher pitch angles stabilize the system. Static simulation results at different suspension preloads suggest that on increasing the preload the desired fly height value decreases, but we need to spin the disk at higher rpm's to attain this fly height.

ACKNOWLEDGMENTS

This work was supported by the Computer Mechanics Laboratory at the University of California, Berkeley.

REFERENCES

[1] Gupta V, Bogy DB, "Effect of Intermolecular Forces on the Static and Dynamic Performance of Air Bearing Sliders: Part I – Effect of initial excitations and slider form factor on the stability," Transactions of the ASME, Journal of Tribology (accepted for publication).

[2] Wu. L., "Physical modeling and numerical simulations of the slider air bearing problems in hard disk drives," Ph.D. dissertation, University of California, Berkeley, 2001

[3] Thornton B.H., "Head-Disk Interface Dynamics of Ultra-Low Flying Air Bearing Sliders for Hard-Disk Drive Applications," Ph.D. dissertation, University of California, Berkeley, 2003

[4] Lin Wu, Bogy DB., "Effect of the intermolecular forces on the flying attitude of sub-5 nm flying height air bearing sliders in hard disk drives," Transactions of the ASME, Journal of Tribology, vol.124, no.3, July 2002, pp.562-7.

[5] Thornton BH, Bogy DB, "Head-disk interface dynamic instability due to intermolecular forces," IEEE Transactions on Magnetics, vol.39, no.5, pt.2, Sept. 2003, pp.2420-2.

[6] B. Zhang, and A. Nakajima, "Possibility of surface force effect in slider air bearings of 100 Gbit/in 2 hard disks," Tribology International, vol. 36, pp. 291-296, April – June 2003.

[7] J. H. Li, B. Liu, W. Hua, and Y. S. Ma, "Effects of intermolecular forces on deep sub- 10 nm spaced sliders," IEEE Trans. Magn , vol. 38, pp. 2141-2143, Sept. 2002.

[8] J. N. Israelachvili, Intermolecular and surface forces, 2nd ed. San Deigo: Academic Press, 1992.

[9] B. H. Thornton, and D. B. Bogy, "Non-Linear Aspects of Air Bearing Modeling and Dynamic Spacing Modulation in Sub 5 nm Air Bearings for Hard Disk Drives," IEEE Transaction on Magnetics, Vol. 39, pp. 722-728, March 2003.

Table 1: Touchdown-takeoff rpm and desired fly height

	Touchdown RPM	Takeoff RPM	Hysterisis in RPM	Desired Fly Height (nm)
$A_1 = 0.5*10^{-19}J$	1500	2900	1400	4.08
$A_2 = 1.0*10^{-19}J$	1900	4400	2500	5.05
$A_3 = 2.0*10^{-19}J$	2700	6500	3800	5.39

Table 2: Touchdown-takeoff rpm's and desired fly height

	Touchdown RPM	Takeoff RPM	Hysterisis in RPM	Desired Fly Height (nm)
ID	2400	5500	3100	6.07
MD	1900	4500	2600	5.07
OD	3000	4500	1500	3.57

Table 3: Touchdown-takeoff rpm's and desired fly height

	Touchdown RPM	Takeoff RPM	Hysterisis in RPM	Desired Fly Height (nm)
Pico w 1.5gm	3000	4500	1500	3.57
Femto w 0.75gm	3000	7000	4000	4.15
Femto w 1.5gm	5800	10500	4700	3.37

Table 4: Touchdown-takeoff rpm's and desired fly height

Suspension Preload (gm)	Touchdown RPM	Takeoff RPM	Hysterisis in RPM	Desired Fly Height (nm)
1.0	1300	3100	1800	4.44
1.5	3000	4500	1500	3.57
2.0	4500	5600	1100	2.95
2.5	5600	6600	1000	2.37
3.0	6800	7600	800	1.87

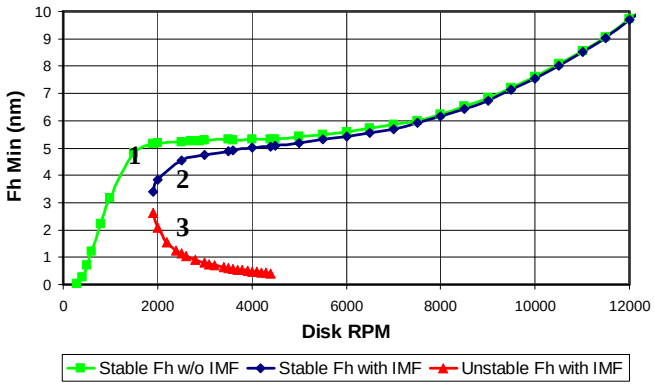

Fig. 1 Fly height diagram

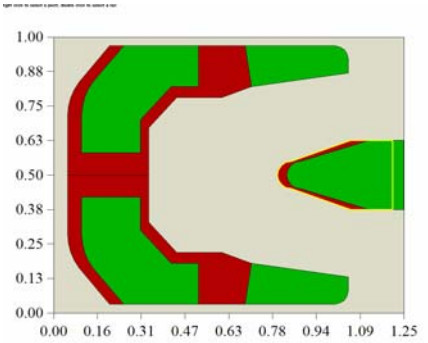

Fig. 2 Pico slider with a crown of 30 nm and a camber of -5 nm. The base recess is 1.397 μm.

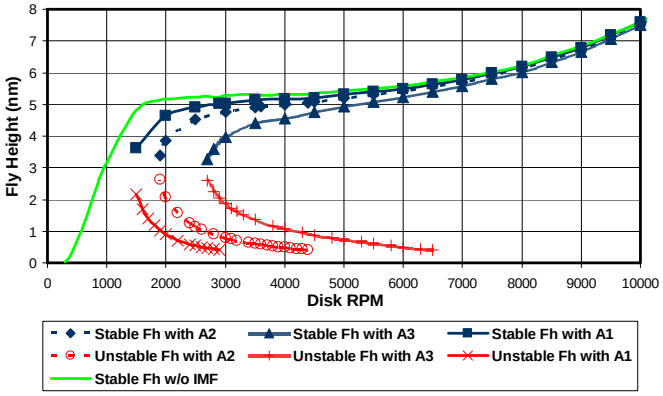

Fig. 3 Fly height diagram with different values of Hamaker constant

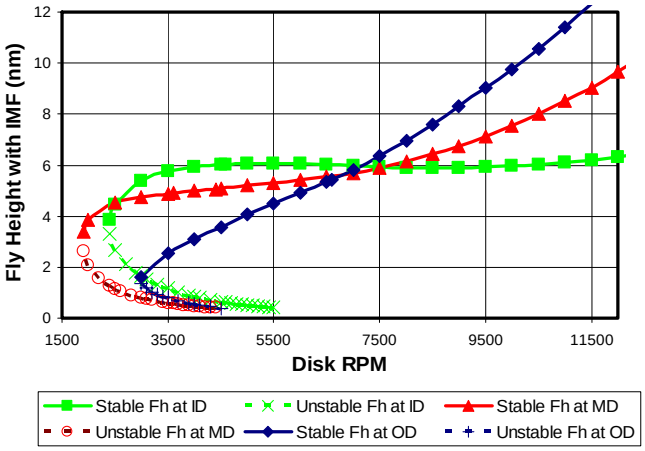

Fig. 4 Fly height diagram for slider shown in fig. 2

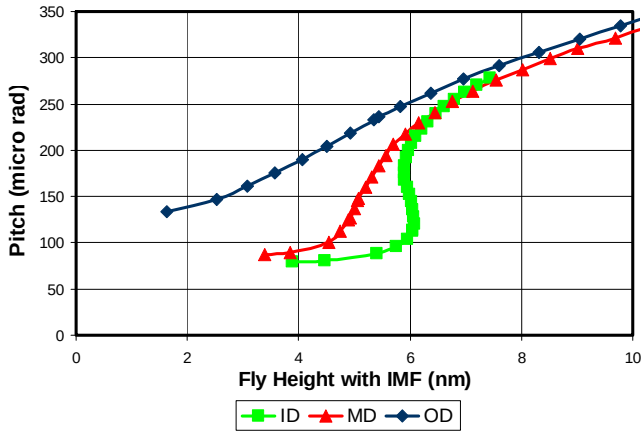

Fig. 5 Pitch versus fly height for slider shown in fig. 2

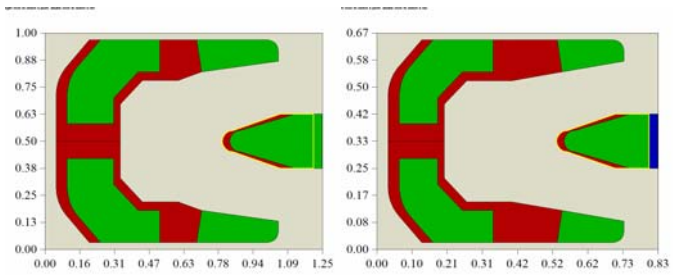

Fig.6 Pico slider with a crown of 25.4nm and a camber of 2.5nm. The base recess is 2.5µm. Femto slider with a crown of 17nm and a camber of 2nm. The base recess is 2.3µm.

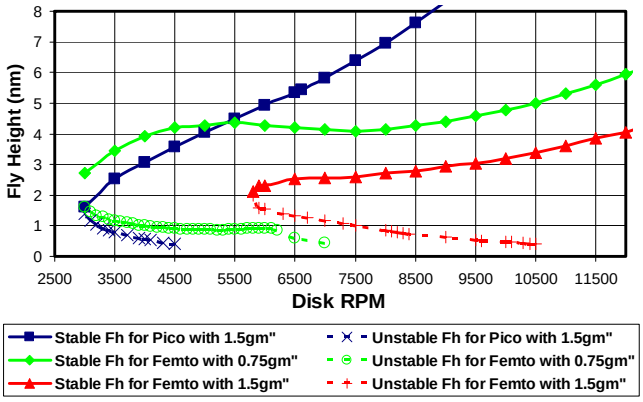

Fig. 7 Fly height diagrams for pico and femto slider designs at different suspension preloads.

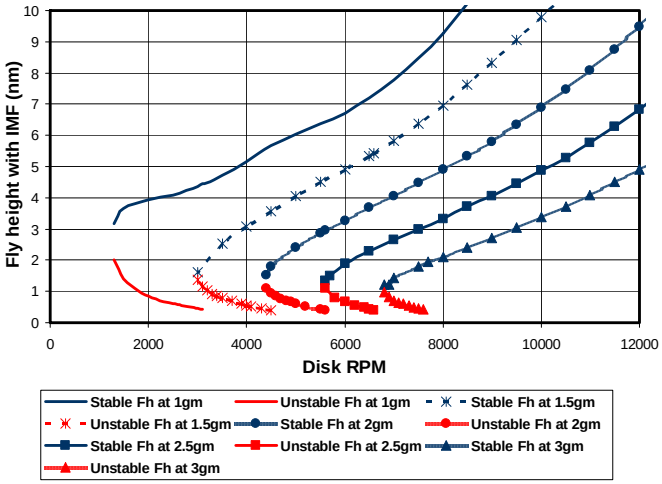

Fig. 9 Fly height diagrams for pico slider design (fig.2) at different suspension preloads.

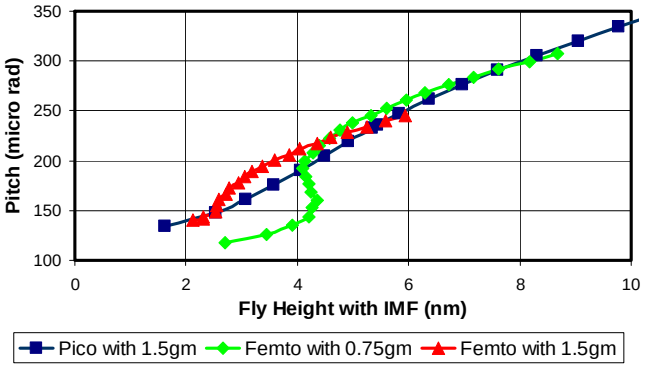

Fig. 8 Pitch versus fly height for sliders shown in fig. 6

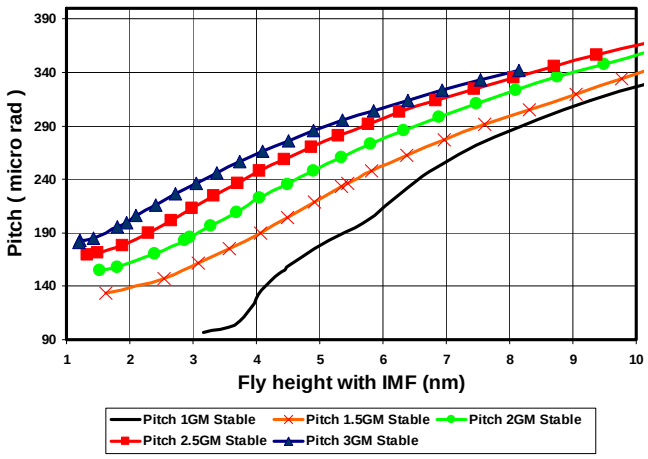

Fig. 10 Pitch versus fly height for sliders shown in fig. 2 at different suspension preloads